1-1-1977

Measurements of 1.5- to 5.3-μm Infrared Enhancements Associated With a Bright Auroral Breakup

K. D. Baker
Utah State University

D. J. Baker
Utah State University

J. C. Ulwick Jr.
Utah State University

A. T. Stair Jr.
Utah State University

Baker, K. D., D. J. Baker, J. C. Ulwick, and A. T. Stair Jr. 1977. "Measurements of 1.5- to 5.3-μm Infrared Enhancements Associated with a Bright Auroral Breakup." *Journal of Geophysical Research* 82 (25): 3518–28. doi:10.1029/JA082i025p03518.

MEASUREMENTS OF 1.5- to 5.3-μm INFRARED ENHANCEMENTS ASSOCIATED WITH A BRIGHT AURORAL BREAKUP

K. D. Baker and D. J. Baker

Utah State University, Logan, Utah 84322

J. C. Ulwick and A. T. Stair, Jr.

Air Force Geophysics Laboratory, Hanscom Air Force Base, Massachusetts 01731

Abstract. A Paiute-Tomahawk sounding rocket containing a 1.5- to 5.3-μm cryogenically cooled spectrometer was flown into a very bright (IBC III$^+$) auroral breakup from Poker Flat, Alaska. The main emission features at 2.8, 4.3, and 5.3 μm were all found to be enhanced owing to the large energy input to the atmosphere associated with the aurora. The most prominent enhancement occurred in the 4.3-μm feature which is identified as emission from the CO_2 (ν_3) band. The maximum of the peak spectral radiance of this feature was observed at a rocket altitude of 92 km and had a value of about 130 MR/μm, which is nearly 2 orders of magnitude greater than that for an undisturbed atmosphere. By comparing upleg and downleg data, it was ascertained that the time constant for this excitation/radiation process is longer than 5 min. It is concluded that the excitation process involves vibrational excitation of nitrogen followed by collisional radiance v-v transfer to CO_2, which then radiates at 4.3 μm. The 5.3- and 2.8-μm features are attributed to radiation from fundamental and first-overtone NO bands.

Introduction

Measurements of infrared auroras have been difficult to make owing to the opacity of the lower atmosphere in the near infrared. However, with the advent of fast and sensitive cryogenic detectors it has been possible to obtain measurements of atmospheric radiations in the 1.5- to 5.3-μm region from aboard rockets which fly above the highly absorbing troposphere. Remarkably bright infrared auroras were seen. These infrared auroral emissions were spectrally analyzed by using a rocket-borne spectrometer flown into a very bright display of visual range aurora. In this paper these observations are reported, and a discussion is given of the processes responsible for the observed infrared enhancements.

Instrumentation

The primary sensor of a Paiute-Tomahawk rocket payload (USAF 10.205-2) flown at Poker Flat, Alaska, on March 24, 1973, was a spectrometer for measurements of auroral emission spectra in the short-wave infrared region (1.5-5.3 μm). The basic characteristics of the spectrometer are summarized in Table 1. As supporting measurements the rocket payload also included a forward viewing diagnostic photometer for monitoring the auroral activity of the region penetrated by the rocket.

The infrared spectrometer [Stair et al., 1973] used a circular variable filter to scan from 1.5 to 5.3 μm at a rate of 2/s (see Figure 1). The spinning filter, an indium antimonide detector, and associated optics were housed in a dewar and cooled to 77°K by a reservoir of liquid nitrogen. The instrument had a 5° full angle field of view directed along the forward vehicle axis. To achieve a wide dynamic range, the instrument was equipped with two linear gain ranges differing by a factor of 10 (low- and high-gain channel).

The photometer, which operated at λ 3914 Å to observe the N_2^+ (0, 0) 1 NG band, was coaligned with the infrared spectrometer. By thus monitoring the auroral activity a means was provided for calculating the energy deposition rate from a measured emission profile. Both optical sensors were uncovered at about 70 km by the ejection of a split clamshell nose cone. The payload itself remained attached to the rocket motor. The rocket was spin-stabilized only, but the aspect was known precisely from the output of an on-board gyro aspect system.

Rocket Flight Summary

Paiute-Tomahawk rocket 10.205-2 was launched at 0031:42 hours Alaskan standard time on March 24, 1973, from the University of Alaska's Poker Flat Research Range near Chatanika, Alaska. The rocket flew to an apogee of 211 km at T + 234 s at a flight azimuth of 049°T. The rocket nose cone was ejected at T + 56 s at an altitude of

TABLE 1. Characteristics of Infrared Spectrometer Aboard Paiute-Tomahawk 10.205-2

Parameter	Value
Wavelength, μm	1.5-5.3
Spectral resolution, %	∿4
Scan rate, Hz	2
Electrical bandwidth, Hz	100
Field of view (full angle), deg	5
Orientation (along forward vehicle axis), deg	0
Minimum detectable signal at 4.3 μm, MR/μm	∿1
Inverse responsivity at 4.3 μm (high gain), MR/μm	14.5

Paper number 7A0578.

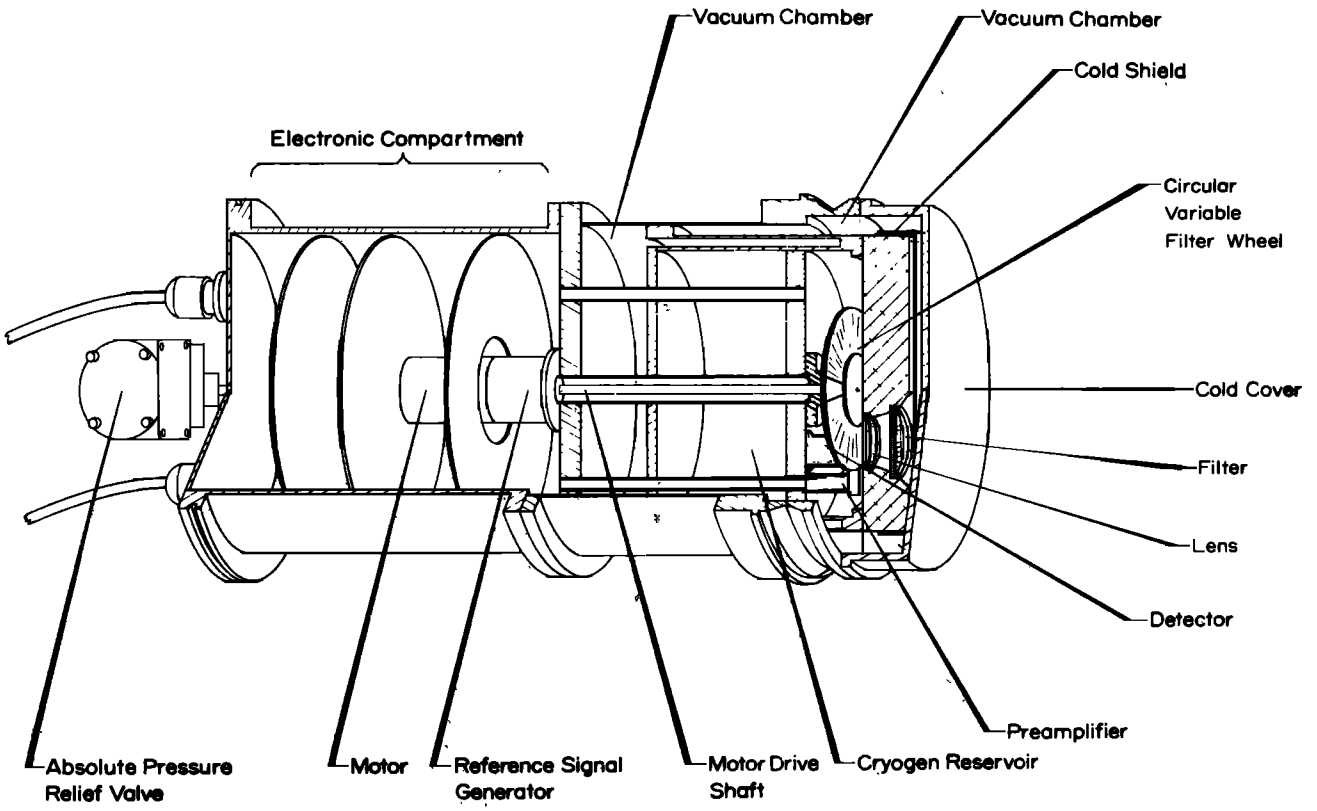

Fig. 1. Liquid nitrogen-cooled infrared circular variable filter spectrometer.

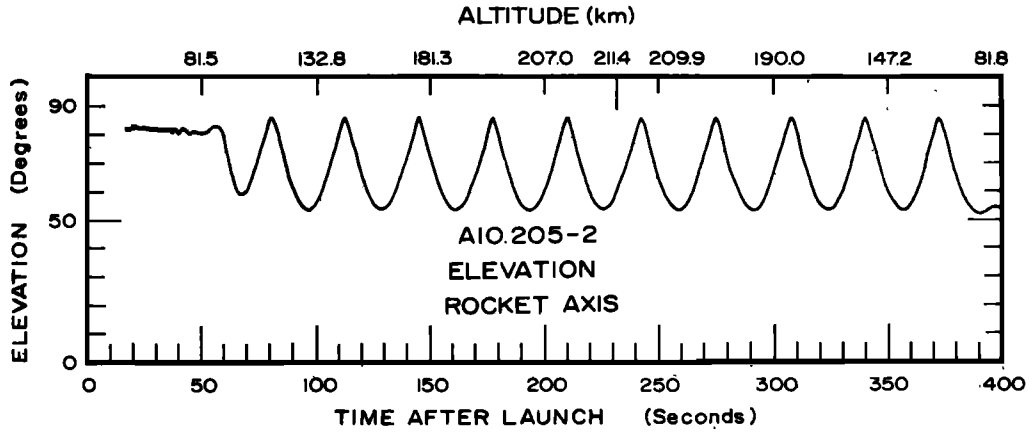

Fig. 2. Elevation of the rocket axis during the flight (Paiute-Tomahawk A10.205-2).

TABLE 2. Geophysical Conditions at Launch

General Condition	Expansion Phase of Auroral Substorm (Intense Breakup)
Maximum auroral brightness penetrated (λ 5577 Å), kR	~500
Estimated energy deposition rate at time of penetration (90 km), ergs/cm^2 s	400
Estimated energy deposited in region for 5 min before rocket penetration, ergs/cm^2	1.5×10^4
Maximum N_e penetrated, el/cm^3	4×10^6
30-MHz riometer absorption, dB	14
Local H magnetic bay, γ	-1000

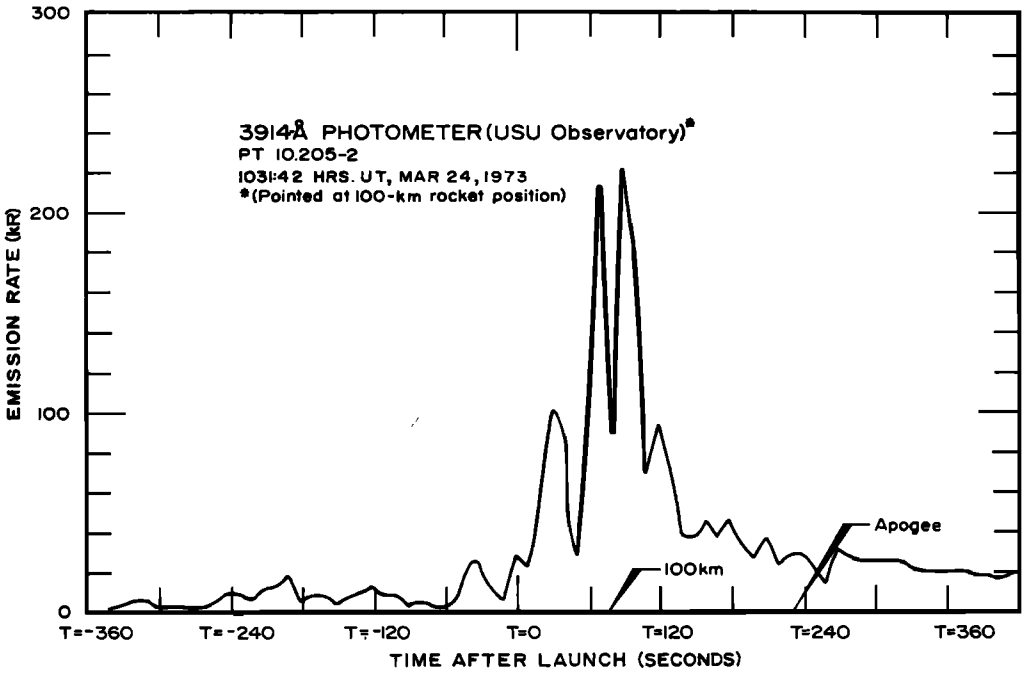

Fig. 3. Ground-based photometer data (λ 3914 Å) for rocket entry position. The rocket times at 100 km on ascent and apogee are indicated.

71 km, exposing the optical instruments at that time.

The rocket roll rate was approximately 6 Hz, and the rocket axis had a precessional motion on a cone of about 16° (half angle) with a period of 33 s. The angle of elevation of the rocket axis is plotted as a function of time in Figure 2 for the duration of the flight. As can be seen, the angle to the vertical of the optical axes of the coaligned instruments went through a range of 4°-36°.

Auroral and Geophysical Conditions

The rocket was launched during an auroral substorm and traversed the initial bright region of the auroral expansion phase in the midnight sector. The extreme brightness of the aurora (∿500 kR of λ 5577 Å), a negative bay in the horizontal component of the terrestrial magnetic field of greater than 1000 γ, the extreme electron density (4×10^6 cm^{-3}), and a large aurorally associated radio frequency absorption (14 dB at 30 MHz) in concert indicate that the rocket penetrated a highly disturbed active region during the auroral breakup expansion. A detailed triangulation analysis of ground-based optical data made in support of the flight was not possible, since the skies were partially cloudy at some of the observation sites. Also, being unstable, the event had extremely fast time fluctuations. Nonetheless, a general picture of the magnitude of the energy deposition of the region traversed by the rocket was deduced. The geophysical conditions associated with the launch are summarized in Table 2.

The time history of the auroral intensity of the region penetrated by the rocket on ascent is perhaps best portrayed by the results shown in Figure 3. These data are from a λ 3914-Å photometer located at the launch site and aimed at the rocket entry point to an altitude of 100 km on rocket ascent. This photometer had a 5° field of view (full angle) centered on a position along the flight azimuth at an elevation angle of 78°. From this vantage point the rocket position would be within the photometer field of view at rocket flight times from about T + 60 s (78 km) to T + 120 s (155 km). More importantly, though, the photometer provided a continuous monitor for a period of minutes before the launch up until the rocket penetration of the auroral activity and particle energy deposition in the auroral region (85-125 km) through which the rocket flew.

The data shown in Figure 3 are for a period of 6 min before launch up through the rocket apogee. The first of the large double peaks with a magnitude of 210 kR occurred at T + 68 s, at which time the rocket was at an altitude of 90 km. Thin clouds over the launch site reduced the measured intensities by a factor that was estimated to be about 2. On the basis of these data it is estimated that a total particle energy of about 1.5×10^4 $ergs/cm^2$ was deposited in the region penetrated by the rocket during the preceding 5 min.

The optical data from the University of Alaska's meridian scanning photometers located at Fort Yukon are shown in Figure 4 for the 100-km rocket entry and exit points. The λ 5577-Å emission rate as seen from this vantage point exceeded 100 kR from shortly after rocket lift-off until the rocket reached an altitude of about 165 km (T + 130 s). In interpreting the results from Fort Yukon, two factors are important: (1) in observing the auroral form the viewing aspect is considerably different from aspects of both the instruments located at Poker Flat and those on board the rocket; and (2) owing to the relatively low elevation angles (29°, 44°), appreciable corrections must be made for optical extinction. The λ 5577-Å emission rates at the rocket entry point (ascent) should be mul-

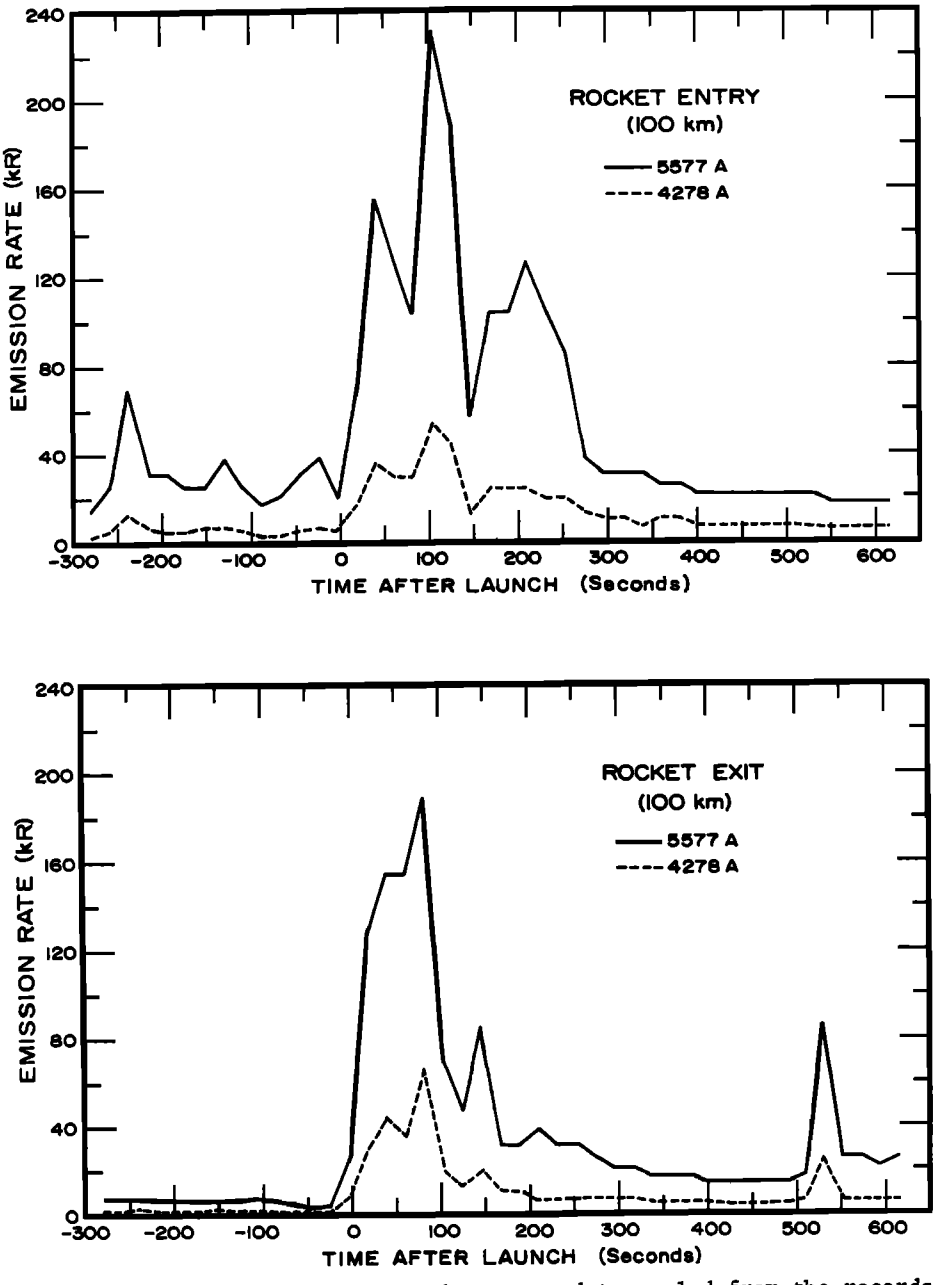

Fig. 4. Fort Yukon meridian scanning photometer data scaled from the records for (top) rocket entry position and (bottom) rocket exit position [Romick, 1974].

tiplied by a factor of about 2 to correct for atmospheric extinction.

The launch of the rocket occurred at the onset of a large negative bay in the horizontal component of the terrestrial magnetic field. A College, Alaska, magnetogram indicated a negative bay of approximately 1000 γ. Magnetometer data from other stations and a more complete description of the magnetic activity and current systems are available from Romick [1974].

The 30-MHz auroral absorption measured by using riometers at College Station reached levels of about 20 dB, indicating that high-energy electron fluxes penetrated low into the ionosphere. During the time of the flight of the rocket the observed absorption was greater than 10 dB.

An incoherent scatter radar located near the Poker Flat Research Range (Chatanika) was operated by the Stanford Research Institute in support of the Icecap rocket measurements program [Baron and Chang, 1975]. These results are particularly useful in the case of the Paiute-Tomahawk flight, since no on-board measurements of electron density and related particle flux data were made. These radar results yield a good picture of the time history of the auroral energy deposition in the region probed by the rocket.

The radar was first operated in a three-spatial position mode, which facilitates electric field and related measurements. Then, shortly before rocket launch (T - 6 min) the radar was fixed on the predicted rocket entry point (elevation, 78.9°; azimuth, 38.7°) to an altitude of 90 km in order to document the electron density and energy deposition in that region during rocket penetration. The measured electron density exceeded 10^6 cm^{-3}

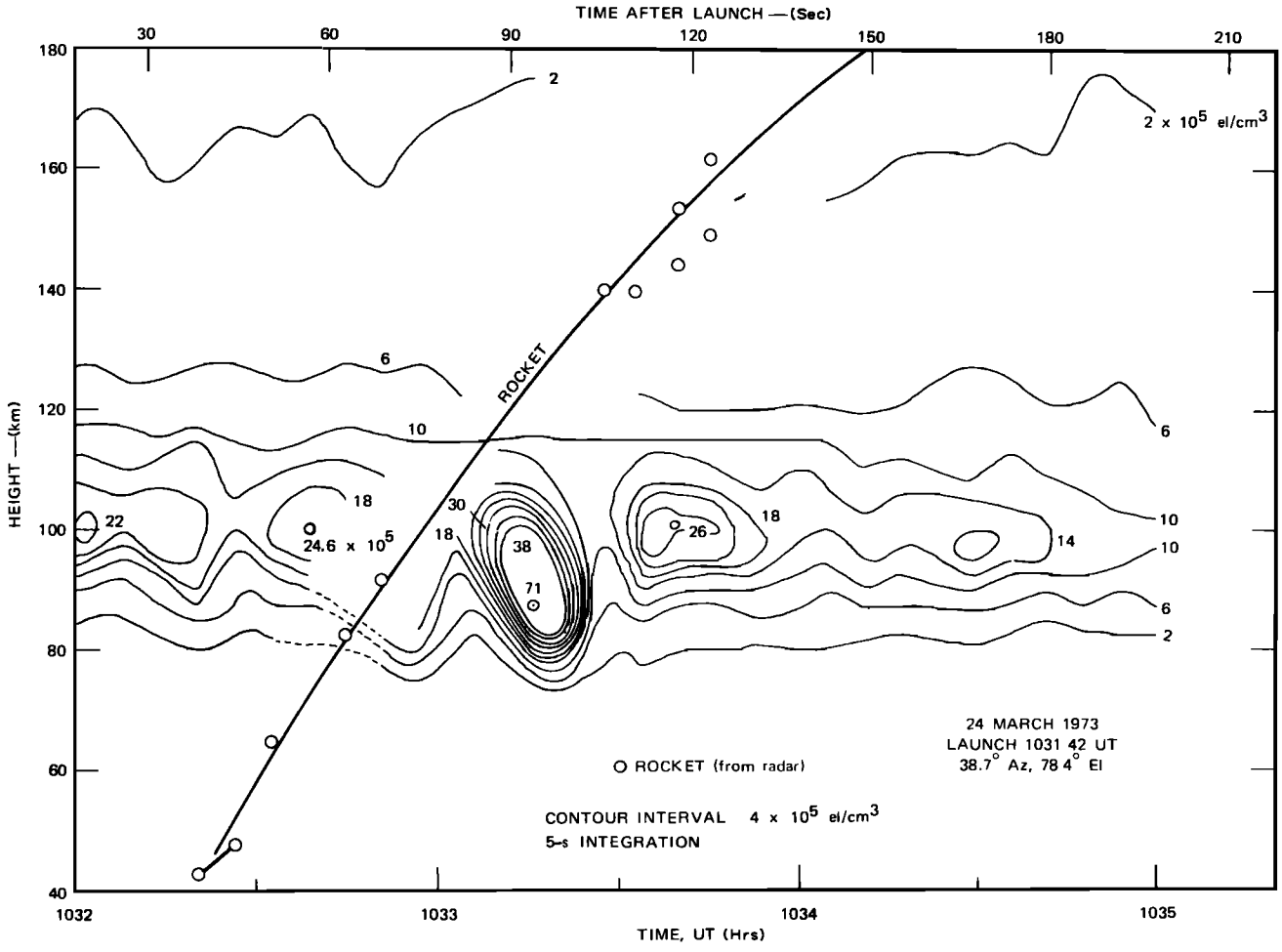

Fig. 5. E-region electron density contours around launch time of Paiute-Tomahawk A10.205-2 [Baron and Chang, 1975].

at 90 km during nearly all of the time that the rocket was on the upleg trajectory. These high electron densities at 90 km indicate that the influx of particles of relatively high energy deposited most of their energy below 100 km.

The conditions during the rocket flight are shown by the electron density contours plotted from radar results in Figure 5 [Baron and Chang, 1975]. These contours were made by using a data integration time of 5 s. An intense region of ionization occurred between 1033:05 (T + 83 s) and 1033:25 (T + 103 s) hours UT from 80 to 100 km. The peak of 7×10^6 cm^{-3} at 1033:15 hours corresponds to an instantaneous energy deposition of about 1800 ergs cm^{-2} s^{-1}.

The electron density data are plotted as height profiles in Figure 6 at reduced integration times (courtesy of M. Baron, Stanford Research Institute). Figure 6 gives the electron density profiles at T + 51 s (63-km rocket altitude) and a composition of data taken at T + 63 s (82-km rocket altitude) and T + 87 s (116 km). This composite was made because the echo from the rocket body contaminates the measurements at the time the rocket passes the altitude of interest. The profiles before and after rocket passage are very similar; it is therefore felt that the composite of Figure 6 gives a valid representation of the electron density distribution penetrated by the rocket. Baron and Chang [1975] detail much more information accumulated during this mission, including clutter maps, conductivities, ion and neutral wind velocities, and energy deposition.

Rocket Results

The rocket penetrated a very bright auroral region on rocket ascent. The results of the forward viewing λ 3914-Å photometer shown in Figure 7 verify that this indeed occurred. This strong emission peaked somewhere in the vicinity of 90 km at an emission rate in excess of 200 kR. The maximum possible output of the photometer corresponded to about 190 kR, so the instrument was unfortunately in saturation from about 80 to 97 km. The corresponding emission rate on rocket descent was about 40 kR.

A typical scan of the infrared spectrometer is shown in Figure 8. This particular scan was observed on the high-gain channel obtained at about 72 km shortly after the spectrometer was uncovered. The spectrometer calibration was used to convert the telemetry voltages to values of spectral radiance in megarayleighs per micrometer. Three prominent emission features are evident at 2.8, 4.3, and 5.3 μm. The 2.8- and 5.3-μm emissions are attributed to NO, whereas the 4.3-μm emission

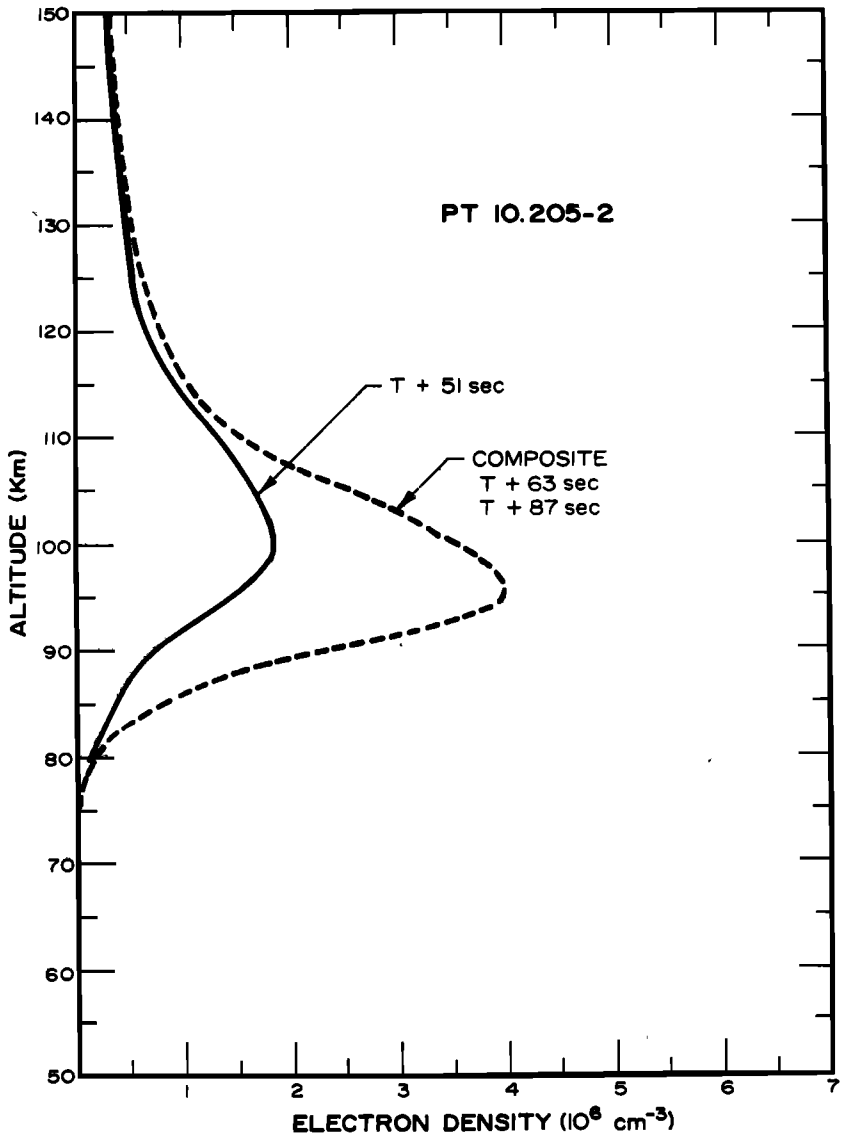

Fig. 6. Electron density profiles from Chatanika radar results.

is identified primarily with CO_2. (See the discussion in the following section.)

The 4.3-μm feature has a width at half amplitude of about 0.16 μm, which is about the resolution element of the spectrometer at that wavelength and also happens to be about the expected width of CO_2 band features. The NO features are not as well measured, since the NO overtone occurs near the seam of the two-segment circular variable filter at about 2.8 μm; also, the longwave spectral cutoff of the InSb detector occurs at about 5.3 μm, which does not include all of the fundamental band.

Figure 9 illustrates both the high- and the low-gain channel outputs of the spectrometer for the spectral scan at about 92 km on rocket ascent. The 4.3-μm feature has brightened significantly over the earlier scan, and the 5.3-μm feature is slightly more intense. Higher altitude scans (98, 106 km) are shown in Figure 10. As the rocket ascends, the 4.3-μm peak drops rapidly, whereas the 5.3-μm feature decreases more gradually.

The peak spectral radiances of the main feature at 4.3 μm were read from the spectral scans, and the results are shown in Figure 11 for rocket ascent. Each point shown represents the reading from each spectral scan of the spectrometer. As the cold cover was removed, the value at about 72 km was 43 MR/μm and decreased with altitude to a minimum at about 77 km, whereupon the value increased to a large peak. This large peak of about 130 MR/μm occurred at about 92 km, where the auroral energy deposition was also maximum. The total measured emission rate in this band, considering the spectral width to be 0.16 μm, is 21 MR. Above the peak of the emission layer the magnitude dropped off to a value of about 5 MR/μm at 110 km. The emission diminished into the background above about 130 km. Also shown in Figure 11 is a profile measured in the absense of auroral activity with a similar infrared sensor flown to 110 km on a Nike Javelin rocket (NJ 74-1) from Poker Flat. This rocket was flown at 0801 hours UT on April 11, 1974. The peak spectral radiance of the 4.3-μm emission at 92 km for the bright auroral case is a factor of 60 brighter than this quiet background value.

A comparison of the 4.3-μm profile measured

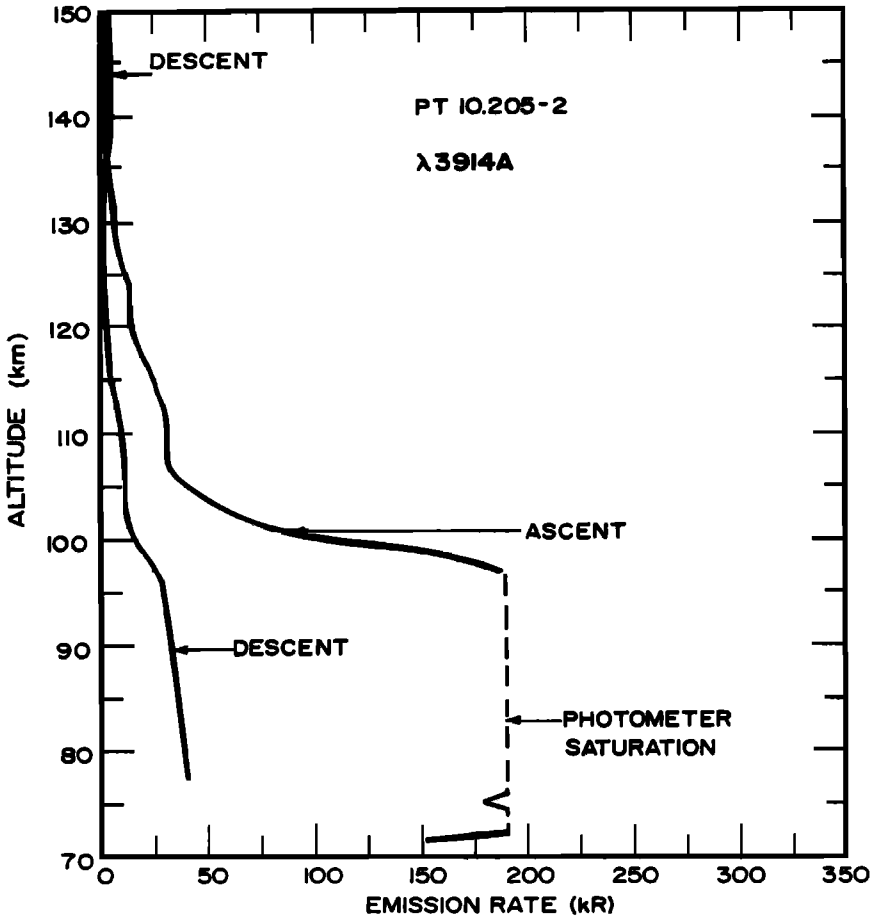

Fig. 7. Data from λ 3914-Å forward viewing rocket photometer. This photometer saturated at 190 kR.

on rocket ascent and descent for the auroral case is shown in Figure 12. It is interesting that although the auroral activity had significantly subsided in the region through which the probe descended (35 kR of λ 3914 Å at 90 km versus over 200 kR on ascent), the peak spectral radiance measured around 90 km had about the same value. Some 330 s elapsed between the 90-km penetration on ascent and descent during which the rocket had moved horizontally to the northeast a distance of 70 km. The implications of the bright region persisting on rocket descent are that the 4.3-μm excitation and emission processes do not closely follow the instantaneous auroral energy input. The infrared emission, in fact, lags in a manner that depends on the time history of the energy input. The decay time constant appears to be longer than the 5 min (the time between upleg and downleg penetration). The emission layer was lower and broader as seen on the rocket descent compared with that observed during ascent. The significance of this could be that there was a net downward diffusion of the excited species.

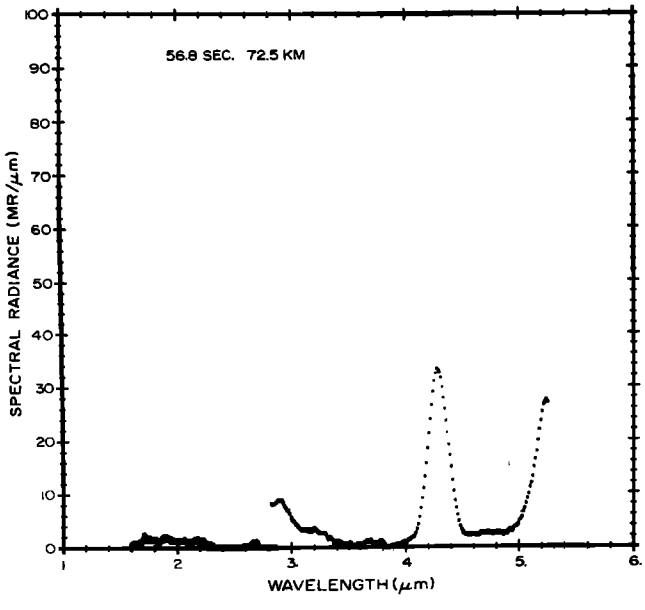

Fig. 8. Infrared spectrometer scans at 72.5 km soon after instrument was uncovered.

The values of peak spectral radiance measured at wavelengths near the location of the circular variable filter junction at 2.8 μm and the high-wavelength cutoff at 5.3 μm are shown in Figure 13. The data points from all usable scans are included; telemetry signal dropout obliterated several scans during the payload descent. Comparisons of rocket ascent and descent data indicate substantial infrared enhancements associated with the strong auroral activity penetrated on rocket ascent. The similarity of the two ascent curves suggests that both radiations arise from

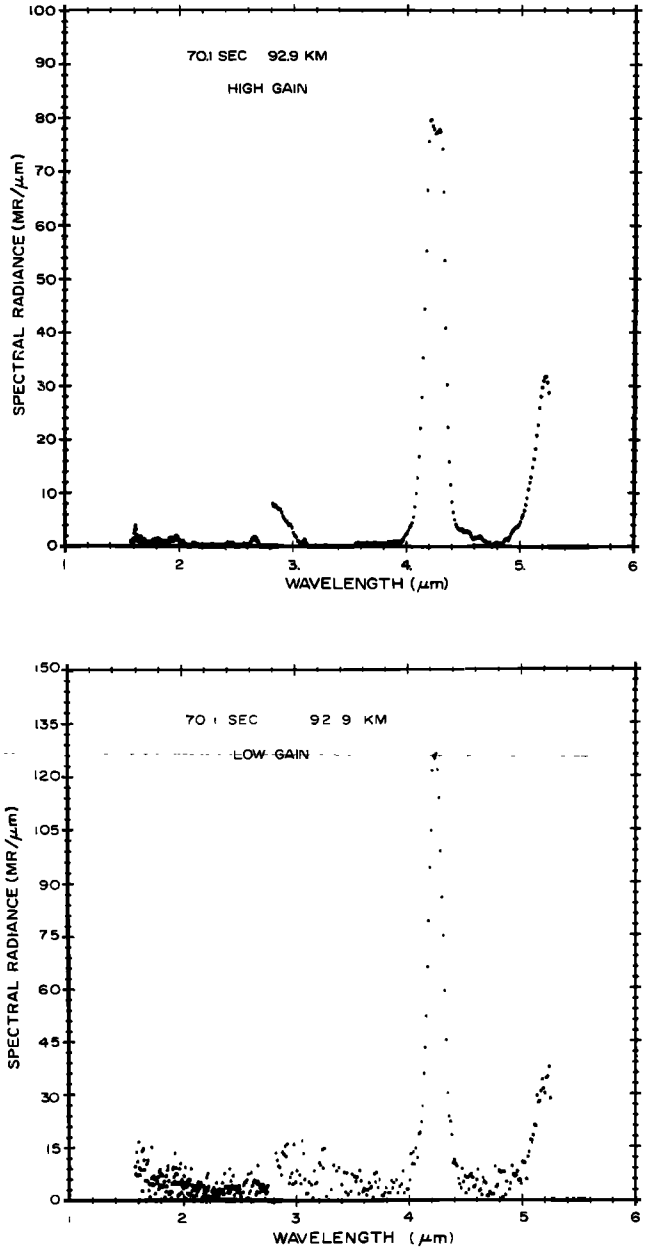

Fig. 9. Spectrometer scans at 92.9 km shown for (top) the high-gain channel and (bottom) the low-gain channel that differ in electronic gain by a factor of 10. The 4.3-μm peak is saturated in the high-gain channel. Note the different vertical scales on the two panels.

the same emitting species, presumably NO. The maximum emissions at these wavelengths were observed between 80 and 90 km but did not show up as a smooth layer and in fact exhibited considerable structure. The increase with altitude of these optically thin emissions and the observed structure suggest that the bright emissions between 80 and 90 km are due to temporal fluctuations rather than simply a low inherent altitude of these emissions compared with the slow 4.3-μm emission. It also is significant that the 2.8-μm emission was essentially absent during the rocket descent at a time of weaker auroral activity.

Discussion

The infrared auroras observed in this rocket experiment were tentatively identified with radiation in the $CO_2(\nu_3)$ band at 4.3 μm and the NO $\Delta v = 2$ and $\Delta v = 1$ bands at 2.8 and 5.3 μm, respectively. The rationale behind these identifications of the likely excitation processes is as follows.

The significant features of the 4.3-μm emission layer were the strong enhancement of infrared radiation associated with a visible bright aurora, the layerlike shape of the measured radiation, and the relatively long time constant for the energy input to infrared emission process. Comparison of the peak spectral radiance measured on this flight with a similar measurement made during an aurorally nondisturbed time [Wheeler et al., 1976] shows that at an altitude of 92 km the

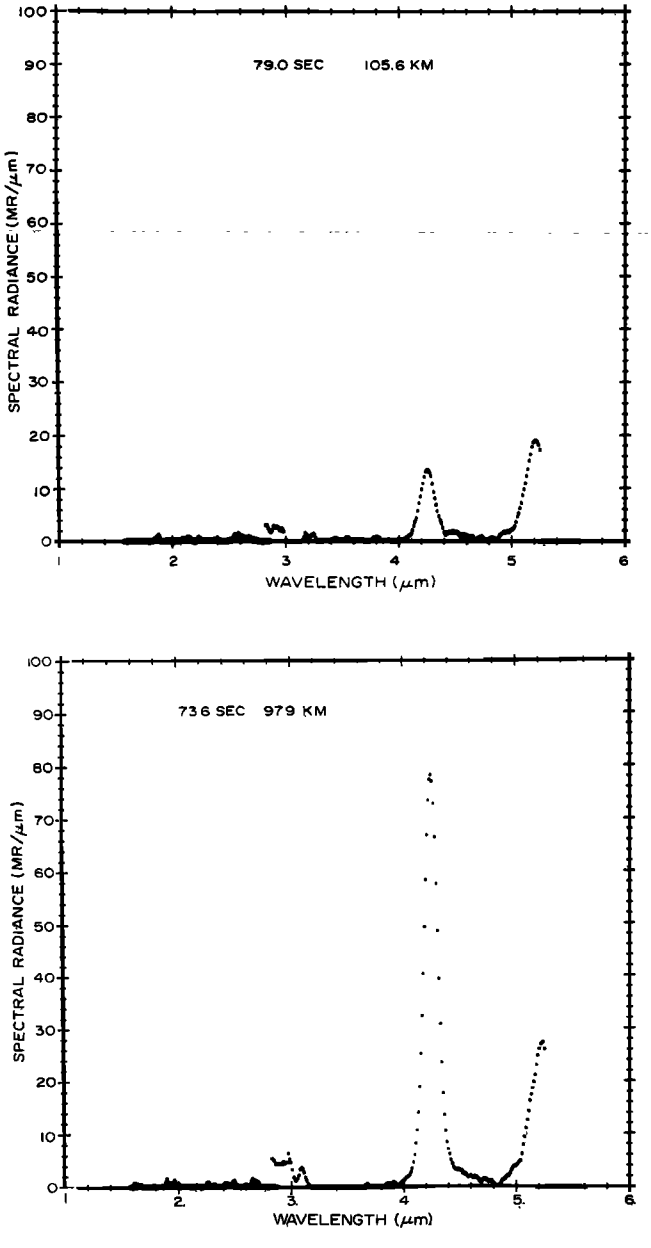

Fig. 10. Spectrometer scans at 97.9 and 105.6 km (high gain).

4.3-μm emission has been enhanced in the auroral case by a factor of about 60.

The observed increase of zenith radiance at 4.3 μm below 92 km as the rocket ascended indicated that the emission region was optically thick. In other words, the observed zenith emission rate is not the integrated total emission along the optical path, as would be the case for optically thin emitters which allow only monotonically decreasing integrated intensity with altitude. The long persistence of the emission (as seen from ascent-descent comparisons) indicates a process for storing energy with a net radiative lifetime greater than 5 min. Both of these characteristics constitute strong evidence that CO_2 is the principal emitter.

Another possible candidate for the 4.3-μm emission would be NO^+ in the $\Delta v = 1$ band. Emission from NO^+ would be expected to closely follow, both temporally and spatially, the instantaneous energy deposition as measured by the onboard N_2^+ (λ 3914 Å) photometer (Figure 7) in this intense auroral case. This conclusion is based upon the knowledge that NO^+ is an optically thin radiator in the atmosphere in the altitude range of the observed 4.3-μm emission layer and that the time constant for the concentration of NO^+ is very short in comparison with the temporal behavior of the observed 4.3-μm radiation. In the region of intense auroral activity encountered during rocket ascent the time constant for the formation or destruction of NO^+ can be approximated by $(\alpha N_e)^{-1}$, where α is the effective dissociative recombination coefficient and N_e is the electron density. Since the electron density was about 4×10^6 cm^{-3} (see Figure 6), the time constant would be about 1 s. An additional factor is that the spectral shape of the NO^+ band should be much broader than that of the observed band, which was of the order of or smaller than the 0.16-μm resolution element. These features of the observed 4.3-μm feature appear to preclude the possibility of a significant contribution of the 4.3-μm emission from NO^+.

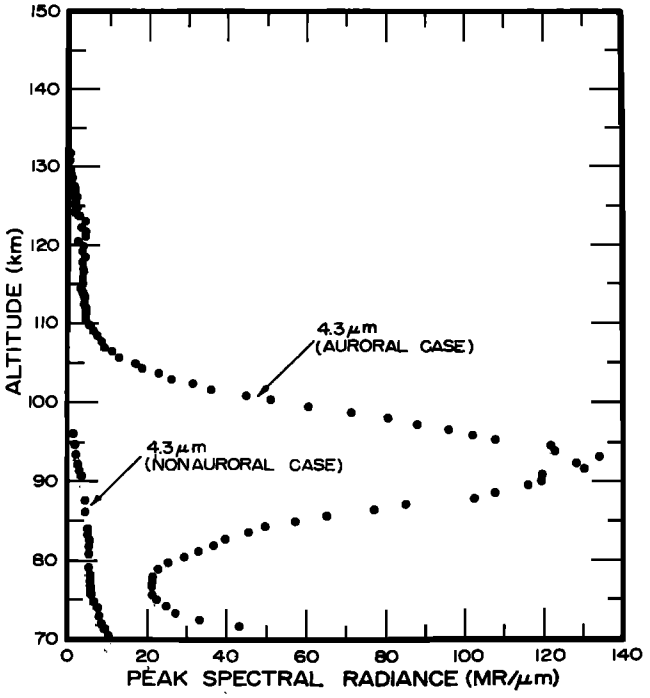

Fig. 11. Peak spectral radiance profile measured at 4.3 μm for the bright aurora. A nonauroral measurement is also shown for comparison.

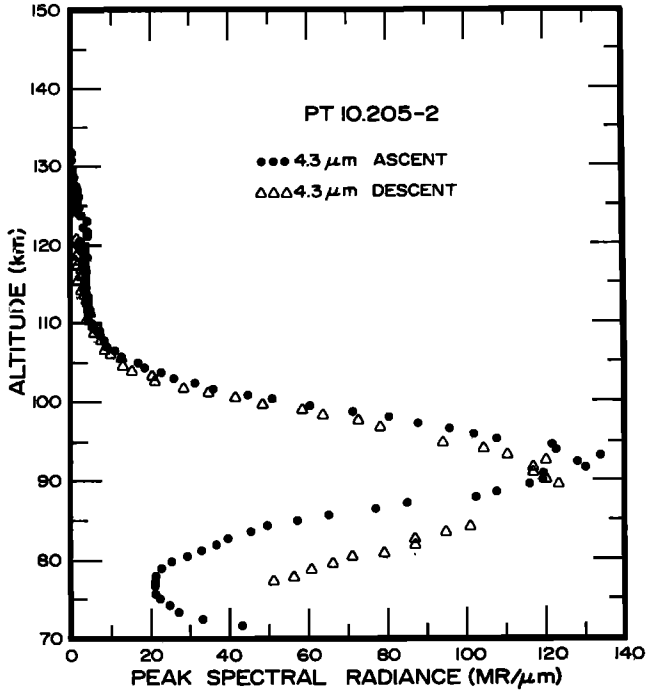

Fig. 12. Comparison of measured 4.3-μm emission profiles for rocket ascent and descent.

The CO_2 excitation mechanism must involve an indirect process, since the cross section for direct excitation of CO_2 by electron bombardment is insufficient to account for the observed brightness of the 4.3-μm emission. The proposed process to model the observations first includes vibrational excitation of N_2 by auroral electrons. The excited N_2 molecules form a reservoir of vibrational energy that can be transferred to CO_2 upon collision, since CO_2 and N_2 have coequal vibrational energy level spacings. This resonant v-v energy transfer is thereby an efficient process for exciting the CO_2 which can then radiate at 4.3-μm. This mechanism is complicated by repeated absorptions and reemissions in the CO_2, since the atmosphere is optically thick to the CO_2 radiation band in the altitude range of maximum emission. It is expected that repeated transfers of vibrational energy back and forth between N_2 and CO_2 by the reversible process $N_2^{\ddagger} + CO_2 \rightleftarrows N_2 + CO_2$ (001) take place. The series of processes are illustrated in Figure 14. Kumer [1974] has shown by a more detailed analysis that the general features of the observed profiles can be explained by such a process, and he derives an efficiency of 15 quanta per ion pair for the production of N_2 vibrational quanta.

The altitude profiles at 2.8 and 5.3 μm which were measured are believed to be due to NO emission that is enhanced over the normal background owing to substantial energy inputs to the atmo-

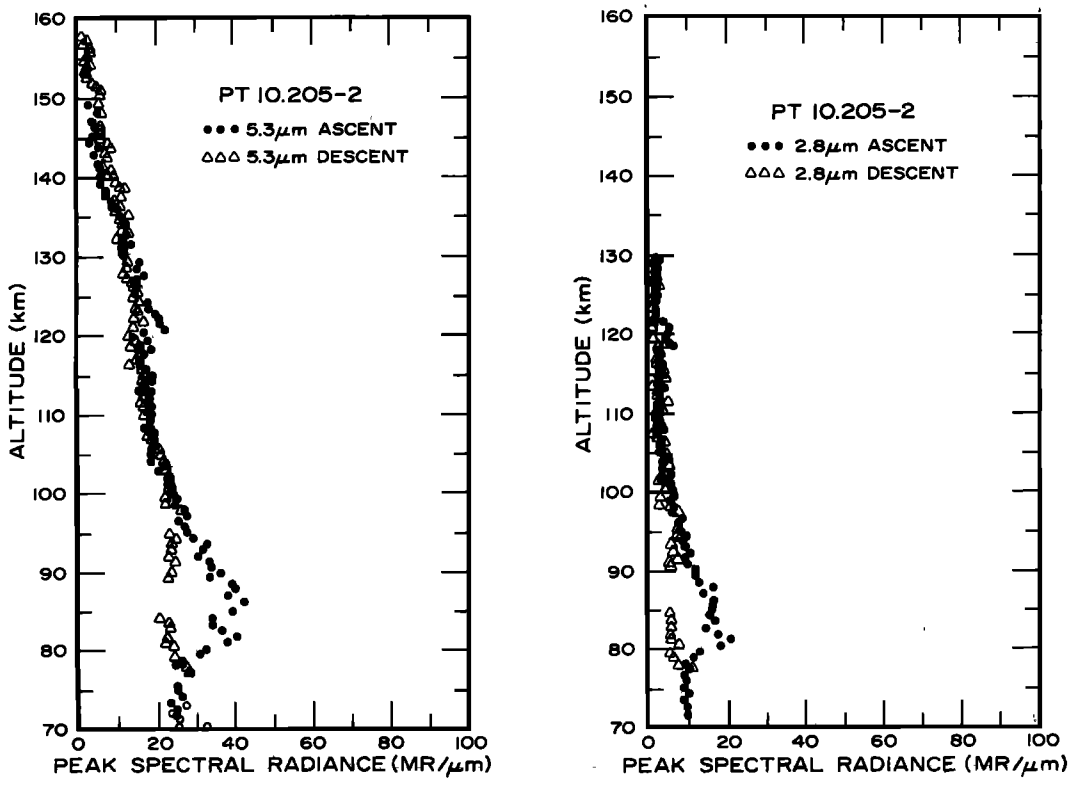

Fig. 13. Magnitude of peak spectral emission (rocket ascent and descent) measured at λ 5.3 and 2.8 μm.

sphere by the auroral event. Comparison with aurorally nondisturbed measurements [Wheeler et al., 1976] indicates that the rocket descent data shown in Figure 13 are approximately at aurorally quiet levels. Under auroral activity the NO is excited by nitrogen-oxygen processes that energetically can excite both the $\Delta v = 1$ and the $\Delta v = 2$ sequences responsible for the observed emissions at 2.8 and 5.3 μm. A principal precursor for these excitation processes is $N(^2D)$, which is produced by a number of electron and ion reactions. From the reactions listed by Reidy et al., [1974] and Oran et al. [1975], perhaps the most important for producing the observed NO emissions are

$$NO^+ + e \rightarrow N(^2D) + O$$

$$N_2 + e\ (fast) \rightarrow N(^2D) + N(^4S)$$

$$N_2^+ + O \rightarrow N(^2D) + O$$

$$N(^2D) + O_2 \rightarrow NO^{\ddagger} + O$$

These reactions will be fast in comparison with the 4.3-μm processes described above. The lower observed altitude of the 5.3-μm emission is believed to be caused by a temporal variation coupled with this faster response time. Comparison of the 5.3-μm profile of Figure 13 (ascent) with the 3914-Å profile of Figure 7 shows a similar temporal increase from 75 to 77 km until the photometer is saturated. The 5.3-μm structure between 80 and 90 km is strongly suggestive of auroral fluctuations, so it is suggested that the peak 5.3-μm of about 86 is representative of an auroral brightening rather than a true layer.

The excitation mechanisms (earthshine and O atom interchange) for NO excitation under nonauroral conditions will not produce radiation at 2.8 μm but do account for the observed background 5.3-μm emission. From the absence of the 2.8-μm emission during the less intense auroral activity, coupled with the similarity of the altitude profile under intense auroral activity, the conclusion is drawn that excited NO ($\Delta v = 2$) is responsible for the auroral enhancement at 2.8 μm.

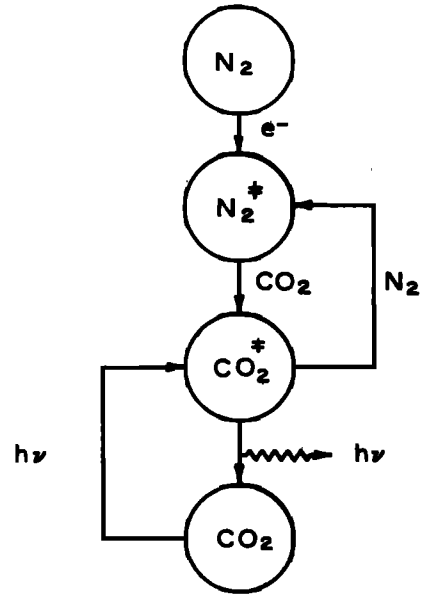

Fig. 14. Schematic representation of excitation/emission processes associated with 4.3-μm aurora.

Acknowledgments. The authors acknowledge the contributions of the staff members of the Defense Nuclear Agency, the Air Force Geophysics Laboratory, Utah State University, Geophysical Institute at the University of Alaska, Stanford Research Institute, and other agencies in the successful accomplishment of this project, which was carried out as part of the Defense Nuclear Agency Icecap program.

The Editor thanks A. Vallance Jones and D. Murcray for their assistance in evaluating this paper.

References

Baron, M. J. and N. J. Chang, Icecap 73A--Chatanika Radar Results, HAES Rep. 15, DNA Rep. 3531T, Stanford Res. Inst., Stanford Univ., Menlo Park, Calif., April 1975.

Kumer, J. B., Analysis of 4.3-μm Icecap data, HAES Rep. 19, AFCRL Rep. TR-74-0334, Lockheed Palo Alto Res. Lab., Palo Alto, Calif., July 1974.

Oran, E. S., P. S. Julienne, and D. F. Strobel, The aeronomy of odd nitrogen in the thermosphere, J. Geophys. Res., 80(22), 3068, 1975.

Reidy, W. P., T. C. Degges, O. P. Manley, H. J. Smith, J. W. Carpenter, A. T. Stair, Jr., J. C. Ulwick, and K. D. Baker, Analysis of HAES results: Icecap 72, Final Report, HAES Rep. 2, DNA Rep. 3247F, Visidyne, Inc., Burlington, Mass., April 1974.

Romick, G. J., Report on the geophysical description and available data associated with rocket PF-PT-54 (PT 10.205-2) report, Univ. of Alaska, Fairbanks, May 1974.

Stair, A. T., N. B. Wheeler, D. J. Baker, and C. L. Wyatt, Cryogenic IR spectrometers for rocket-borne measurements, in IEEE/NEREM 1973 Record, part 3, Infrared, Institute of Electrical and Electronics Engineers, New York, 1973.

Wheeler, N. B., A. T. Stair, Jr., D. G. Frodsham, and D. J. Baker, Rocket-borne spectral measurement of atmospheric infrared emission during a quiet condition in the auroral zone, AFGL Rep. TR-76-0252, Environ. Res. Pap. 583, HAES Rep. 32, Air Force Geophys. Lab., Hanscom Air Force Base, Mass., October 1976.

(Received April 1, 1977;
accepted June 15, 1977)